

An experimental study of the contact mode AFM scanning capability of polyimide cantilever probes

Angelo Gaitas*, Yogesh B. Gianchandani

Department of Electrical Engineering and Computer Science, University of Michigan, 1301 Beal Avenue, Ann Arbor, MI 48109, USA

Received 6 August 2005; accepted 14 December 2005

Abstract

This paper presents a preliminary exploration of high-speed contact mode performed with a polyimide probe. The probe is batch micromachined by a lithographic manufacturing process. It offers a spring constant of <0.1 N/m, a resonance frequency of about 50 kHz, and a tip diameter of 50–100 nm. The probe is particularly suitable for scanning soft specimens such as biological and polymeric samples. Topographical contact mode imaging at high scanning rates of 48 Hz (1.47 mm/s) has been demonstrated, detecting features <100 nm over a $15\ \mu\text{m}$ scan, yielding >7 bit resolution at 48 Hz. Scanning rates of 16 Hz (0.5 mm/s) have been demonstrated for lateral force imaging with spatial resolution of 100 nm over a $15\ \mu\text{m}$ scan, which translates into >7 bit resolution at 16 Hz. These results suggest that the probe can be used in high throughput applications.

© 2006 Elsevier B.V. All rights reserved.

Keywords: Atomic force microscopy; Failure analysis; Scanning thermal microscopy; Scanning probe microscopy; Lateral force measurements; Frictional force measurements; High speed imaging; High throughput

1. Introduction

Scanning probe methods developed within the last two decades offer high-resolution images of sample properties. First introduced by Binnig et al. [1] in 1986, scanning probe microscopes (SPM) measure properties such as topographical variations, thermal conductance, temperature, capacitance, optical absorption, frictional forces, or magnetic field, at localized spots. The SPM has been a very successful research tool. However, till recently it offered limited throughput. Scan speeds of current tapping mode AFMs are limited to about 180–250 $\mu\text{m/s}$ due to actuation time constant of the piezo-electrically actuated feedback loop [2,3]. A typical value for contact mode imaging is about 75 $\mu\text{m/s}$ [4].

A number of approaches have been reported for faster image acquisition: (a) *Scanning at constant height with no feedback*: This method creates variations of the imaging force. However, unintended contact between the tip and the sample can be damaging to both [5]. (b) *Using high*

frequency piezo segments for out-of-plane movement of the probe along the z-axis [6–9]. While this method is effective, it limits the dynamic range that can be accommodated in the topographical variation [5]. (c) *Integrating actuators on the probe to reduce the mass that has to be moved*: Several groups have worked on cantilevers and cantilever arrays with integrated piezo-actuators allowing direct force control through the cantilever and imaging in parallel [10–17]. At first, electrical crosstalk between the actuator and piezoresistor signals at high-frequency operation was observed. This was partially addressed using a lock in amplifier and an AC bridge circuit for each cantilever [14]. However, this creates significant challenges when scaling up to multi-probe systems. In addition, while ZnO actuators have been capable of producing results at 4 mm/s [2,14], they have a high-leakage current [2], and their maximum deflection is relatively low, at about 3 μm at several tens of applied voltage [2]. Furthermore, with commercially available piezoresistive cantilevers, a user generally gives up an order of magnitude of force resolution [18].

Cantilevers for frictional force measurements typically use Si_xN_y or Si as structural materials. However, they do

*Corresponding author. Tel.: +734 763 6032.

E-mail address: agaitas@umich.edu (A. Gaitas).

not necessarily offer the best compromise in material properties, and can necessitate the use of demanding fabrication steps or complex structures [19,20]. Sensitivity to frictional forces depends on the ratio of Young’s modulus to the shear modulus. Comparing the ratios suggests that polyimide is more appropriate than either Si or Si_xN_y for cantilevers used in lateral force measurements. Further, the lower Young’s modulus of polyimide allows for improved imaging of soft samples.

We have previously reported scanning thermal probes fabricated by 6- to 7-mask surface micromachining processes using polyimide as the shank material, and the application of these probes for temperature mapping, sub-surface imaging, and the measurement of glass-transition temperature in photoresists [21–24]. The probes have also been used for maskless, submicron thermochemical patterning of photoresist [25], hot-spot detection [26], and microfluidics related work, namely for high-speed liquid pumping, mixing and particle entrapment in thin layers of oil and water [27,28]. The probes can be arrayed into an multi-probe system for higher throughput large area scanning [29].

This paper presents an initial exploration of high-speed contact mode topography and lateral force scans performed with ultracompliant polyimide probes (Fig. 1). In the following text, Section 2 provides a brief analysis of polyimide as a structural material, and Section 3 describes the fabrication of the probes and experimental results obtained.

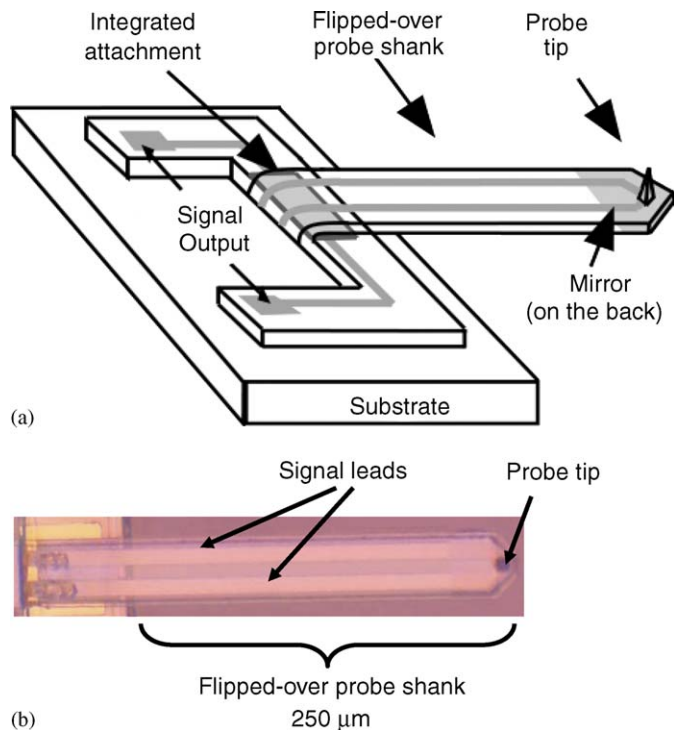


Fig. 1. (a) Schematic drawing of the probe die including the probe cantilever and tip [24]. (b) Optical micrograph of a flipped-over probe shank.

2. Theory

In this section, polyimide is examined as a structural material for cantilevers used in lateral force measurements. Atomic force microscopes are capable of measuring, simultaneously and separately, lateral and normal forces on a cantilever [30]. The topographical image is derived by observing the normal forces and the lateral image by observing the torsional movements of the cantilever, i.e. the twisting of the cantilever (Fig. 2). In lateral force microscopy (LFM) a four-segment photo-diode is used to measure both normal and torsional bending of the cantilever.

As noted in Section 1, the sensitivity to lateral forces depends on material properties, namely the shear modulus and Young’s modulus, as well as the dimensions of the cantilever. The shear modulus of Si_xN_y is 119 GPa and of Si is 80 GPa while polyimide has a shear modulus of 1–10 GPa. The Young’s modulus of the polyimide used in this work is 7.5 GPa compared to 180–300 GPa for Si_xN_y and 130 GPa for Si.

The torsional stiffness of a cantilever beam of rectangular cross-section (without accounting for the tip height) is given by the following equation [31]:

$$K_t = \frac{GWt^3}{16L} \left[\frac{16}{3} - 3.36 \frac{t}{W} \left(1 - \frac{t^4}{12W^4} \right) \right], \quad (1)$$

where G is the shear modulus and W , L and t are the width, the length and the thickness of the cantilever, respectively. Assuming $W \gg t$, this equation can be simplified to

$$K_t = \frac{GWt^3}{3L}. \quad (2)$$

In order to examine the torsional stiffness of the entire probe (cantilever beam and probe tip) another equation has to be used for the torsional spring constant $K_{T,h}$, which includes the effect of scanning tip of height h [19,32]:

$$K_{T,h} = \frac{GWt^3}{3Lh^2}. \quad (3)$$

The typical torsional stiffness of commercial lateral force cantilevers is 50–200 N/m [33]. Using the above equations, Table 1 compares various commercial probes, some of

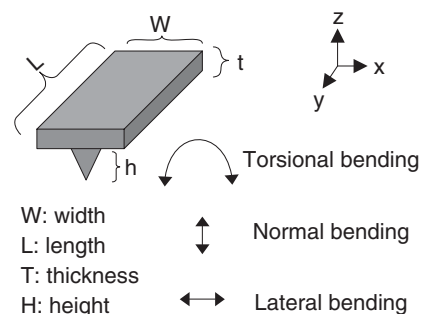


Fig. 2. xyz coordinates and bending modes of the probe cantilever.

Table 1

Comparison of various commercial probes including probes designed for LFM. It can be seen the torsional stiffness of the polyimide probe is considerably lower

	Shear modulus (GPa)	Length (μm)	Width (μm)	Thickness (μm)	Tip height (μm)	Normal bending constant K_B (N/m)	Lateral bending constant K_{LB} (N/m)	Torsional stiffness K_T ($n\text{Nm/rad}$)	Torsional stiffness $K_{T,h}$ (N/m)
Polyimide probe	1–10	250	50	3	7.5	0.082	45	1.8	32
Silicon nitride (Si_3N_4) [34]	119	100	40	0.8	2.9	0.39	2304	8.12	965
Silicon (Si) [35]	80	450	30	2	17.5	0.1	19.3	14.22	46
Silicon nitride (Si_3N_4) [36]	119	100	40	0.5	3.5	0.26	1440	1.98	162

which are specially designed for LFM imaging. It can be seen that the torsional stiffness of the polyimide probe is considerably lower. This is true despite the fact that in its current manifestation the polyimide probe has larger thickness than the commercially available probes. Fig. 3 shows the torsional stiffness obtained using Eq. 3 as a function of length and width of the polyimide probe and of a Si_xN_y probe. The values of two other commercially available probes are included in the graph. The actual value for the polyimide probe was calculated to be 32 N/m, which is lower than other options.

Additional parameters of relevance include the lateral bending spring constant K_{LB} that describes the bending of the cantilever in the x -direction (as defined in Fig. 2) and normal bending spring constant K_N that describes the bending of the cantilever in the y -direction. These two bending constants are given by the following equations [32]:

$$K_{L,B} = \frac{F_L}{\Delta x} = \frac{EW^3 t}{4L^3}, \quad (4)$$

$$K_N = \frac{F}{\Delta z} = \frac{EWt^3}{4L^3}, \quad (5)$$

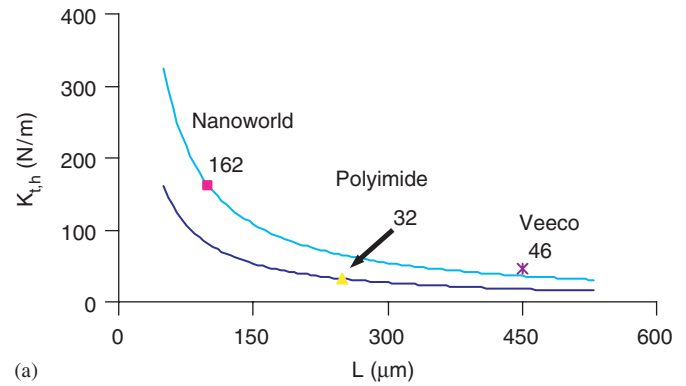
where F and F_L are the applied forces, Δz and Δx are the tip deflections, E is the Young's modulus, W is the width, L is the length, and t is the thickness.

The ratios of the torsional stiffness (including probe tip height) $K_{T,h}$ to the normal force spring constant K_N and to the lateral bending K_{LB} are an indicator of sensitivity to frictional forces. Smaller ratios are preferred. These equations show a linear dependence on the shear modulus and an inversely proportional relationship to the Young's modulus, and also show that shorter, wider cantilevers with longer tips are favorable [32]:

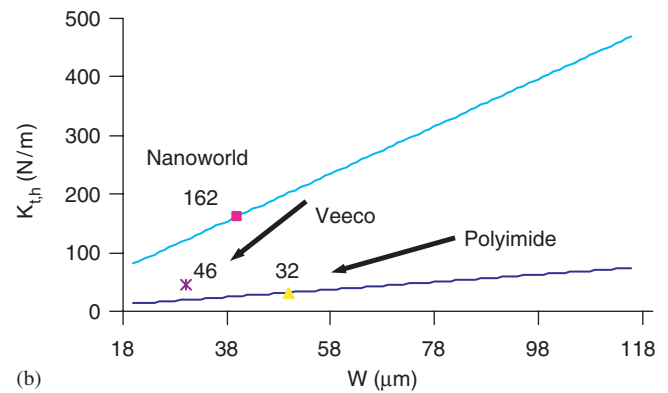
$$\frac{K_{T,h}}{K_{LB}} = \frac{4GL^2 t^2}{3Eh^2 w^2}, \quad (6)$$

$$\frac{K_{T,h}}{K_N} = \frac{4GL^2}{3Eh^2}. \quad (7)$$

For this specific case, when applying the above formulas, the polyimide probe has the lowest ratio of torsional compliance over normal compliance (Table 2). In the general case, if dimensions are equal, the sensitivity ratios



(a)



(b)

Fig. 3. Behavior of torsional stiffness of three different types of probes as a function of length (a) and width (b). The actual value for the polyimide probe is 32 N/m while for the probes marketed by Veeco and Nanoworld, the values are 46 and 162 N/m, respectively.

Table 2

Sensitivity ratios of torsional compliance over lateral compliance, and of torsional compliance over normal compliance

	Ratio of $K_{T,h}/K_{LB}$	Ratio of $K_{T,h}/K_N$
Polyimide probe	0.7111	390
Silicon nitride (Si_3N_4) [34]	0.4193	2477
Silicon nitride (Si_3N_4) [36]	0.1124	623
Silicon (Si) [35]	2.4113	464

are a function of the shear modulus and the Young's modulus of the material. Comparing the ratios suggests that polyimide is favorable for cantilevers used in frictional

force measurements (Table 3). Further, polyimide has a lower normal compliance, which is very advantageous for scanning soft samples.

Table 3
Sensitivity ratios when dimensions are equal are a function of the ratio of the shear modulus over the Young's modulus of the material

	Shear modulus G (GPa)	Young's modulus E (GPa)	Ratio of $G/E \sim K_{T,h}/K$
Polyimide	1	7.5	0.13
Silicon nitride (Si_3N_4)	119	180	0.66
Silicon (Si)	80	130	0.62

3. Experimental results

The structure of the polyimide probe is illustrated in Fig. 1. The probe tip has a diameter of 100 nm, which can be reduced about 50 nm with oxide sharpening. It offers topographical resolution of <1 nm and a spring constant of <0.1 N/m. The tip height is $8 \mu\text{m}$, and the cantilever is $250 \mu\text{m}$ long, $50 \mu\text{m}$ wide, and $3 \mu\text{m}$ thick. The resonance frequency was measured at 50 kHz. The probes are batch fabricated in a process described below. A flip-over assembly step eliminates wafer dissolution. The cantilever is made of two layers of polyimide that sandwich a thin wire of Cr/Au (100 nm thick, $1 \mu\text{m}$ wide), which also serves as a sensing element. The tip is also made of Cr/Au.

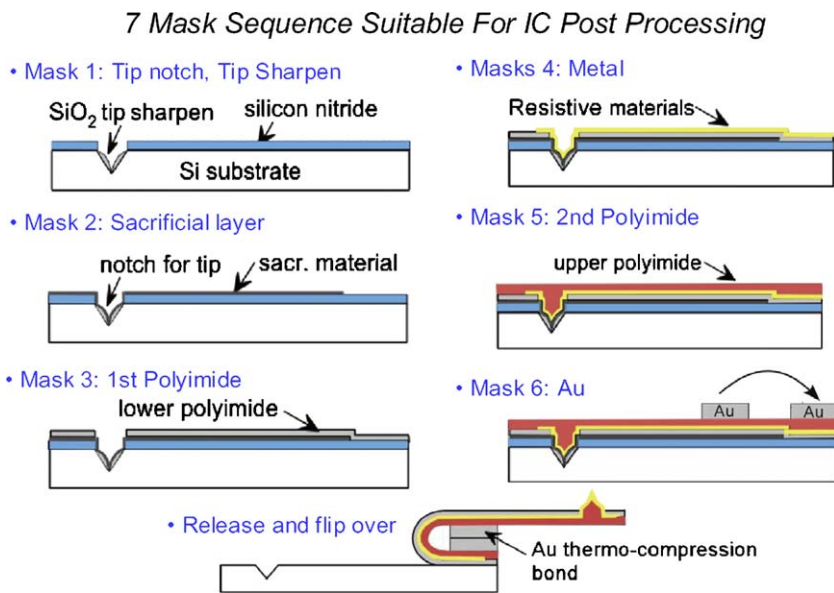


Fig. 4. Fabrication sequence requires 6 masks and is suitable for merging with a CMOS process. An optional mask is typically added after mask 4 when fabricating embedded bolometers or thermocouples in the probe [22–24].

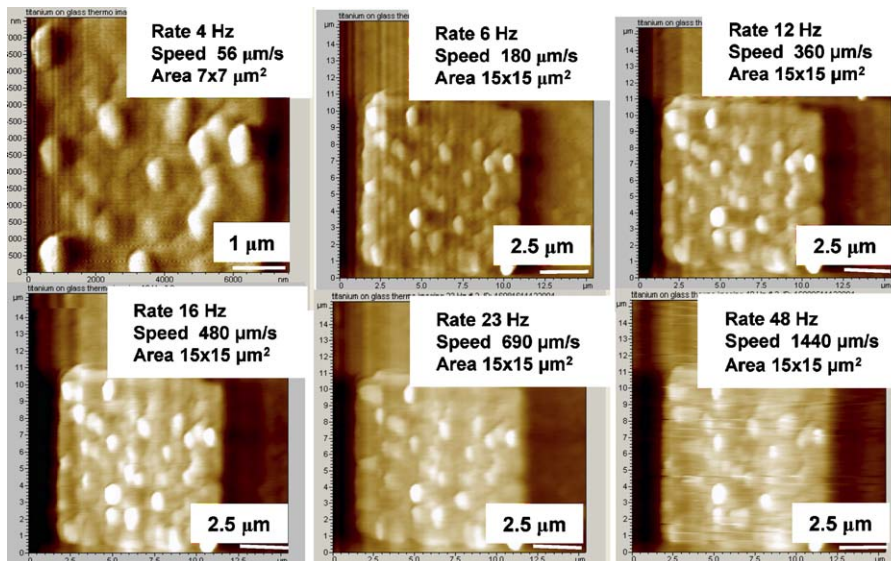


Fig. 5. Force (deflection) images are shown with increasing scanning rates. The sample was 20 nm thick Ti patterned on Pyrex™ glass. The scans were obtained with a PicoMaps system from Molecular Imaging, Inc.

Fig. 4 illustrates the seven masking step fabrication sequence that is suitable for merging with a CMOS process. First, a mold is created for the tip by anisotropic wet etching on a (100) Si substrate. The sacrificial layer is deposited and patterned, followed by the lower polyimide. The metals are then deposited and patterned. Later, the second polyimide layer is deposited and patterned, followed by a gold layer, which will be used for thermocompression

bonding and will also serve as a mirror. Finally, the probe is released, flipped over and held in place by a thermo-compression bond. The maximum fabrication temperature encountered is 350 °C for curing the polyimide.

Several high-speed force images were obtained with the polyimide probe. It has been demonstrated that it is possible to detect features <100 nm over a 15 μm line at 48 Hz (1444 μm/s). Fig. 5 shows scans of force images

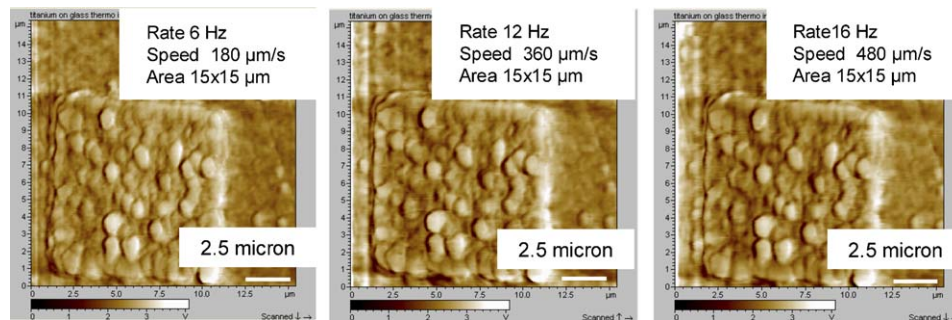


Fig. 6. A number of lateral force scans were obtained. The sample was a 20 nm thick film Ti patterned on Pyrex glass. High resolution images were obtained at up to 16 Hz. The scans were obtained with a PicoMaps system from Molecular Imaging Inc.

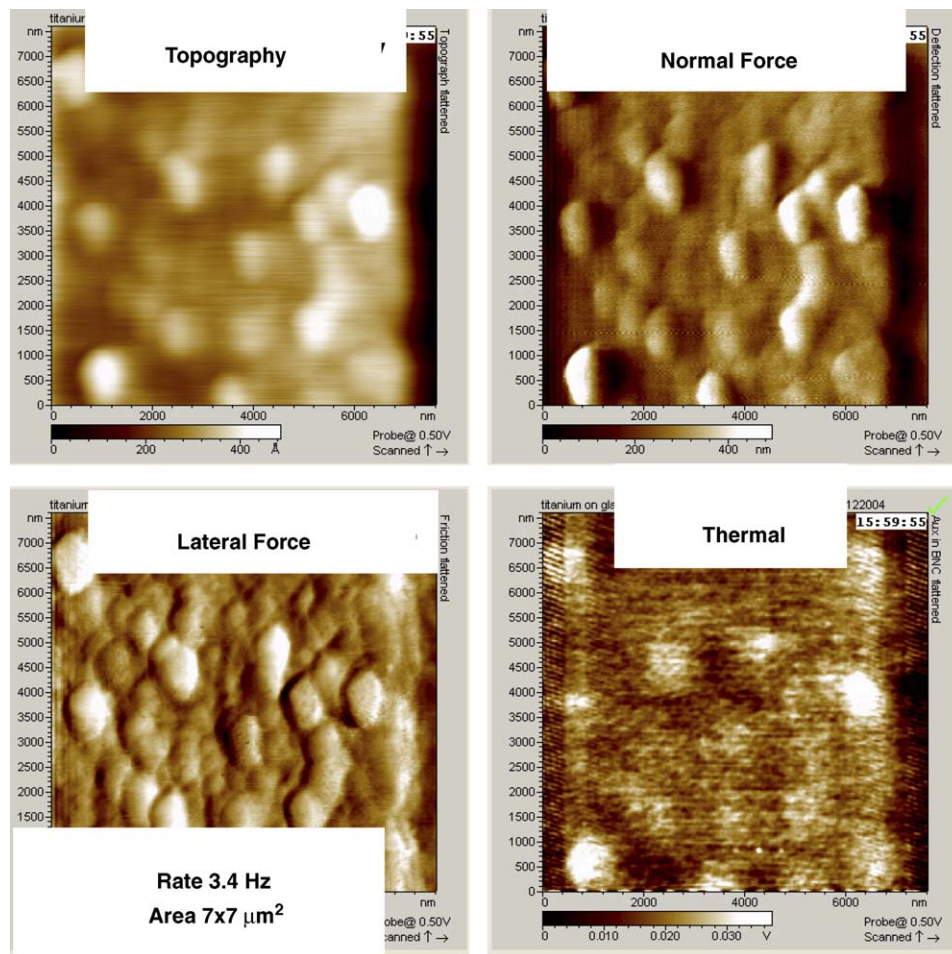


Fig. 7. This figure illustrates topography, lateral force, normal force, and thermal images can be obtained simultaneously. The sample was a 20 nm thick film Ti patterned on Pyrex glass. Thermal features smaller than 200 nm can be observed. The scans were obtained with a PicoMaps system from Molecular Imaging Inc.

(deflection images) with increasing scanning rates. The sample was a 20 nm thick film Ti patterned on PyrexTM glass. The scans were obtained with a PicoMaps system offered by Molecular Imaging, Inc. Although there is some loss of resolution at higher speeds, the image is still visible at 48 Hz (1476 $\mu\text{m/s}$).

In lateral force imaging mode high resolution images were obtained at up to 16 Hz (480 $\mu\text{m/s}$) with a resolution <100 nm over a 15 μm line at 16 Hz. Fig. 6 shows a number of lateral force scans. The sample used was a 20 nm thick film Ti patterned on Pyrex glass.

Fig. 7 illustrates topography, frictional force, and thermal images obtained simultaneously. For these, the PicoMAPS system was used along with the PicoSPM II microscope and the PicoScan 3000 controller. These were connected to the probes through a custom interface circuit that included a Wheatstone bridge, gain stages, and low-pass filters to reduce noise. The output voltage change represents the thermal conductance of the sample. The thermal image deteriorates more rapidly with increasing scanning rates. However, at scan rates of 16 Hz (480 $\mu\text{m/s}$) 1 μm thermal features are still visible. Prior work has shown that with the open-loop interface circuit such as the one used in this experiment thermal data rates in excess of 1 kHz can be accommodated [24]. With servo-controlled circuits higher speeds are acceptable.

4. Conclusion

This effort has addressed applications of a polyimide probe in high-speed normal force and lateral force imaging. Experimental results demonstrate that normal force images can be obtained at 48 Hz (1.47 mm/s) and lateral force images can be obtained at 16 Hz (0.5 mm/s), both with <100 nm spatial resolution over a 15 μm scan (>7 bit resolution). The properties of polyimide suggest that it is favorable for cantilevers used in lateral force measurements. The probe includes a thin film metal resistor as the sensing element for thermal imaging. The probes are fabricated by a 6-mask surface micromachining process. Typical probe dimensions are 250 μm length, 50 μm width, and 3 μm thickness. The probe has a spring constant of 0.082 N/m, and can be further reduced by reducing the probe width and thickness. The probe has a topographical resolution of <1 nm. Furthermore, these probes can easily be arrayed for even higher throughput [29].

Acknowledgments

The authors thank Dr. Song Xu for his help with AFM scans, Molecular Imaging, Inc. for providing with the SPM used in these experiments, Mr. Amar Basu for his help with thermal scans, and PicoCal, Inc. for providing probes.

References

- [1] G. Binnig, C. Quate, C. Gerber, Atomic force microscope, *Phys. Rev. Lett.* 56 (9) (1986) 930–933.
- [2] Y.-S. Kim, H.-J. Nam, S.-M. Cho, J.-W. Hong, D.-C. Kim, J.-U. Bu, PZT cantilever array integrated with piezoresistor sensor for high speed parallel operation of AFM, *Sensors Actuators A* 103 (2003) 122–129.
- [3] R. Pedrak, T. Ivanov, K. Ivanova, T. Gotszalk, N. Abedinov, I.W. Rangelow, Micromachined atomic force microscopy sensor with integrated piezoresistive sensor and thermal bimorph actuator for high-speed tapping-mode atomic force microscopy phase-imaging in higher eigenmodes, *J. Vac. Sci. Technol. B* 21 (2003).
- [4] R.W. Stark, G. Schitter, A. Stemmer, Velocity dependent friction laws in contact mode atomic force microscopy, *Ultramicroscopy* 100 (2004) 309–317.
- [5] G. Schitter, P. Menold, H.F. Knapp, F. Allgower, A. Stemmer, High performance feedback for fast scanning atomic force microscopes, *Rev. Sci. Instrum.* 72 (8) (2001).
- [6] R.V. Lapshin, O.V. Obyedkov, Fast-acting piezoactuator and digital feedback loop for scanning tunneling microscopes, *Rev. Sci. Instrum.* 64 (1993) 2883.
- [7] D. Knebel, M. Amrein, K. Voigt, R. Reichelt, A fast and versatile scan unit for scanning probe microscopy, *Scanning* 19 (1997) 264.
- [8] A. Egawa, N. Chiba, K. Homma, K. Chinone, H. Muramatsu, High-speed scanning by dual feedback control in SNOM/AFM, *J. Microsc.* 194 (2–3) (1999) 325–358; A. Egawa, N. Chiba, K. Homma, K. Chinone, H. Muramatsu, *J. Microsc.* 194 (1999) 325.
- [9] H.J. Mamin, H. Birk, P. Wimmer, D. Rugar, High-speed scanning tunneling microscopy. Principles and applications, *J. Appl. Phys.* 75 (1994) 161.
- [10] S.C. Minne, S.R. Manalis, C.F. Quate, Parallel atomic force microscopy using cantilevers with integrated piezoresistive sensors and integrated piezoelectric actuators, *Appl. Phys. Lett.* 67 (1995) 3918–3920.
- [11] S.R. Manalis, S.C. Minne, C.F. Quate, Atomic force microscopy for high speed imaging using cantilever with integrated actuator and sensor, *Appl. Phys. Lett.* 68 (1996) 871–873.
- [12] T. Itoh, J. Chu, I. Misumi, K. Kataoka, T. Suga, New dynamic scanning force microscopes using piezoelectric PZT microcantilevers in: 1997 International Conference on Solid-State Sensors and Actuators, *Dig. Tech. Papers* 1 (1) (1997) 459–462.
- [13] M. Tortonese, H. Yamada, R.C. Barrett, C.F. Quate, Atomic force microscopy using a piezoresistive cantilever, in: International Conference on Solid-State Sensors and Actuators, 1991 pp. 448–451.
- [14] S.C. Minne, G. Yaralioglu, S.R. Manalis, J.D. Adams, J. Zesch, A. Atalar, C.F. Quate, Automated parallel high-speed atomic force microscopy, *Appl. Phys. Lett.* 72 (1998) 2340–2342.
- [15] Y. Su, A. Brunnschweiler, A.G. Evans, G. Ensell, Piezoresistive silicon V-AFM cantilevers for high-speed imaging, *Sensors Actuators* 76 (1999) 139–144.
- [16] T. Sulchek, S.C. Minne, J.D. Adams, D.A. Fletcher, A. Atalar, C.F. Quate, D.M. Adderton, Dual integrated actuators for extended range high speed atomic force microscopy, *Appl. Phys. Lett.* 75 (11) (1999).
- [17] Y.S. Kim, H.-J. Nam, S.-M. Cho, D.-C. Kim, J.-U. Bu, A Self-Actuating PZT Cantilever Integrated with Piezoresistor Sensor for AFM with High Speed Parallel Operation, Technical Digest, in: MEMS 2002 IEEE International Conference. 15th IEEE International Conference on Micro Electro Mechanical Systems, (2002) pp. 689–692.
- [18] J.A. Harley, Advances in piezoresistive probes for atomic force microscopy, Dissertation, Stanford University, 2000.
- [19] M. Kageshima, M.H. Ogisso, H.S. Nakano, S.M.A. Lantz, M.A. Tukumoto, Atomic force microscopy cantilevers for sensitive lateral force detection, *Japan. J. Appl. Phys.* 38 (6B) (1999) 3958–3961.

- [20] B.W. Chui, T.W. Kenny, H.J. Mamin, B.D. Terris, D. Rugar, Independent detection of vertical and lateral forces with a sidewall-implanted dual-axis piezoresistive cantilever, *Appl. Phys. Lett.* 72 (11) (1998) 1388.
- [21] J.-H. Lee, M.-H. Li, Y.B. Gianchandani, Photoresist metrology and microcalorimetry using an ultracompliant micromachined scanning thermal probe, in: *International Workshop On Thermal Investigations Of ICs and systems (THERMINIC 2002)*, October 2002. Madrid, Spain, pp. 111–116, October 2002.
- [22] M.-H. Li, Y.B. Gianchandani, Microcalorimetry applications of a surface micromachined bolometer-type thermal probe, *J. Vac. Sci. Technol. B* 18 (6) (2000) 3600–3603.
- [23] M.-H. Li, J.J. Wu, Y.B. Gianchandani, Surface micromachined polyimide scanning thermocouple probes, *J. Microelectromech. Syst.* 10 (1) (2001) 3–9.
- [24] M.-H. Li, Y.B. Gianchandani, Applications of a low contact force polyimide shank bolometer probe for chemical and biological diagnostics, *Sensors Actuators A* 104 (2003) 236–245.
- [25] A. Basu, S. MNamara, Y.B. Gianchandani, Scanning thermal lithography: maskless, submicron thermochemical patterning of photoresist by ultracompliant probes, *J. Vac. Sci. Technol. B* 22 (6) (2004).
- [26] E. Hendaro, A. Altes, R. Heiderhoff, J.C.H. Phang, L.J. Balk, Investigation on the thermal distribution of nMOSFETs under different operation modes by scanning thermal microscopy, in: *2005 IEEE International Reliability Physics Symposium, Proceedings 43rd Annual*, 2005, pp. 294–299.
- [27] A.S. Basu, Y.B. Gianchandani, High speed microfluidic doublet flow in open pools driven by non-contact micromachined thermal sources, *Proceedings of the IEEE International Conference on Micro Electro Mechanical Systems*, Miami Beach, FL, 2005, pp. 666–669.
- [28] A.S. Basu, Y.B. Gianchandani, Trapping and manipulation of particles and droplets using micro-toroidal convection currents, in: *Proceedings of the 13th International Conference on Solid-State Sensors, Actuators, and Microsystems*, Seoul, Korea, 2005.
- [29] S.S. McNamara, A.S. Basu, J.-. Lee, B. Gianchandani, Ultracompliant thermal probe array for scanning non-planar surfaces without force feedback, *J. Micromech. Microeng.* 15 (2005) 237–243.
- [30] G. Meyer, N.M. Amer, Simultaneous measurement of lateral and normal forces with an optical-beam-deflection atomic force microscope, *Appl. Phys. Lett.* 57 (20) (1990) 2089–2091.
- [31] W.C. Young, R. Budynas, *Roark's Formulas for Stress and Strain*, McGraw-Hill, New York, sixth ed., p. 348 (1989).
- [32] B.B. Bhushan (Ed.), *Handbook of Micro/Nano Tribology*, Second Ed., 1999.
- [33] R.W. Carpick, D.F. Ogletree, M. Salmeron, Lateral stiffness: a new nanomechanical measurement for the determination of shear strengths with friction force microscopy, *Appl. Phys. Lett.* 70 (12) (1997).
- [34] OMCL-RC800PSA-W, www.olympus.co.jp/en/insg/probe/img/catalog05E.pdf
- [35] MPP-32100—Light Contact Mode Silicon Probes, www.veecoprobes.com
- [36] NanoWorld Hybrid-Nitride™.